Measuring the lateral size of liquid-exfoliated nanosheets with dynamic light scattering

Mustafa Lotya[1,2], Aliaksandra Rakovich[3], John F. Donegan[1,2] and Jonathan N Coleman[1,2*]

[1]*School of Physics, Trinity College Dublin, Dublin 2, Ireland*

[2]*Centre for Research on Adaptive Nanostructures and Nanodevices (CRANN), Trinity College Dublin, Dublin 2, Ireland*

[3]*Department of Physics, Imperial College London, London, UK*

**colemaj@tcd.ie*

We have developed an in-situ method to estimate the lateral size of exfoliated nanosheets dispersed in a liquid. Using standard liquid exfoliation and size-selection techniques, we prepared a range of dispersions of graphene, MoS_2 and WS_2 nanosheets with different mean lateral sizes. The mean nanosheet length was measured using transmission electron microscopy (TEM) to vary from ~40 nm to ~1 μm. These dispersions were characterised using a standard dynamic light scattering (DLS) instrument. We found a well-defined correlation between the peak of the particle size distribution as outputted by the DLS instrument and the nanosheet length as measured by TEM. This correlation is consistent with the DLS instrument outputting the radius of the sphere with volume equal to the mean nanosheet volume. This correlation allows the mean nanosheet length to be extracted from DLS data.

1. Introduction

Over the last few years, 2-dimensional materials have been among the most investigated of nano-materials. Much of the early research focused on graphene due to its unique properties and vast potential for applications.[1] There has also been a sustained interest in layered oxides, largely because of their diversity as well as their usefulness in a range of areas.[2] More recently, attention has begun to turn to other 2-dimensional materials such as BN, MoS_2 and other transition metal chalcogenides. MoS_2, in particular, is a very

* Corresponding Author. Fax: +35316711759, Tel: +35318963859, email: colemaj@tcd.ie (J.N. Coleman)

promising material with much potential both for applications[3] and for the study of novel physical phenomena.[4]

In many cases, early research into 2-dimensional materials relied on mechanically cleaving monolayers from layered crystals.[5, 6] However, it has come to be accepted that many layered materials will be important in applications, for example as fillers in composites,[7, 8] which require large quantities of exfoliated 2-dimensional nanosheets. Large scale exfoliation can be achieved by sonicating layered crystals in appropriate liquids.[7, 9] This process generates large quantities of 2-dimensional nanosheets that are stabilised against aggregation by interactions with the liquid. This can be achieved in certain solvents,[7, 9-24] surfactant[25-31] or polymer solutions[32, 33] where the stabilisation mechanisms are enthalpic, electrostatic and steric respectively.[34] Alternatively, both graphene and inorganic layered materials can be exfoliated by lithium intercalation based methods to give nanosheets,[35-37] while graphene can be exfoliated and dispersed in liquids as graphene oxide.[38, 39]

Once the exfoliated nanosheets have been dispersed in liquids, it is important to know their dimensions. Nanosheets often consist of multiple stacked monolayers so knowledge of thickness can be important. In addition, the nanosheet length often depends on the processing method and must be measured before use.[23] Some applications depend strongly on the nanosheet dimensions. For example, nanosheets are often used as fillers in composites with the aim of improving mechanical,[8, 40] electrical[41] or barrier properties[42]. In each case, the composite performance is sensitive to the nanosheet dimensions. Thus, access to simple methods to measure nanosheet thickness and length is very important.

Measurements of the dimensions of nanosheets from liquid systems are generally crude and indirect. For example, both length and thickness are often measured by atomic force microscopy (AFM) or transmission electron microscopy (TEM).[23, 41] Such methods are tedious and can be inaccurate due to nanosheet aggregation during deposition from the dispersion. It would be far superior to have an in-situ method of analysing the nanosheets dimensions in the liquid dispersion. While some in-situ methods do exist, they require specialist equipment, are time consuming or require complex analysis. Examples of these include laser diffraction and X-ray scanning sedimentation.[43] Other techniques such as size exclusion chromatography and field flow fractionation can be used to assist in the

separation of particles of a given size, however a separate size measurement technique is still required.[44, 45]

The goal of this work is to develop a simple, fast, in-situ method to measure the lateral size of dispersed nanosheets. Such a method should be straightforward and use equipment which is commonly available. In fact, a number of instruments are widely available which can measure the size of colloidal particles using dynamic light scattering (DLS). The simplest way to do this is to measure the particles diffusion coefficient which can be used to infer its size via the Stokes-Einstein relation (see below). However, while this works extremely well for spherical objects, it is less reliable for non-spherical geometries e.g. rods or platelets. For such non-spherical objects, the relationship between the diffusion coefficient and dimension can be relatively complex.[46] As a result, analysis can be complicated and the errors considerable. We believe a simpler approach would be to find a semi-empirical correlation between the size outputted by the DLS instrument (assuming spherical geometry) and the platelet lateral size as measured independently, for example using statistical TEM. To do this it will be necessary to measure the nanosheet size using both DLS and TEM for a range of samples of dispersed nanosheets, each with a different mean nanosheet lateral size. The TEM data could then be used to calibrate the DLS data.

It is known that liquid exfoliation of layered materials, such as graphite, BN or MoS_2, in solvent or water/surfactant systems produces nanosheets with a wide distribution of lateral sizes ranging from tens of nanometres to a few microns.[7, 23, 24, 26-28, 35, 47, 48] Recently, we showed that nanosheet dispersions can be fractionated using a controlled centrifugation regime to select subsets of these nanosheets with varying mean nanosheet sizes.[15, 47] In this work we apply this size selection technique to dispersions of graphene in the solvent N-methyl-2-pyrrolidone (NMP) and an aqueous surfactant solution as well as exfoliated MoS_2 and WS_2 in the solvents NMP and N-cyclohexyl-2-pyrrolidone (CHP) respectively. In this way, for each nanosheet type, we generated 7-10 dispersions, each with a different mean nanosheet length. For each dispersion, we used statistical TEM analysis to assess the sizes of the nanosheets. In addition, we used DLS to measure the hydrodynamic radius of the dispersed objects. We found a well-defined correlation between TEM-measured nanosheet length and DLS-measured hydrodynamic radius. This correlation is consistent with the hydrodynamic radius being proportional to the radius of a sphere whose volume is equal to that of the nanosheets. This correlation can then be used to extract the real nanosheet length from the DLS data.

2. Experimental Methods

All layered materials, i.e. natural flake graphite powder, powdered molybdenum disulphide and powdered tungsten disulphide, were purchased from Sigma Aldrich. The dispersants, i.e. sodium cholate (SC), HPLC grade N-methyl-2-pyrrolidone (NMP) and N-cyclohexyl-2-pyrrolidone (CHP) were also purchased from Sigma Aldrich. All materials were used as supplied. In this study stock dispersions of exfoliated nanosheets were prepared by horn tip sonication (Vibracell CVX 750W) of layered compounds in the appropriate liquid. In all cases cooling was via an ice water bath. Both the graphene/NMP and MoS_2/NMP stock dispersions were prepared by sonicating 40 mg/ml of layered material in 100 ml NMP for 2.5 hrs at an amplitude set-point of 75%. The graphene/SC stock was prepared using 5 mg/ml graphite in 100 ml of a 0.1 mg/ml aqueous SC solution, processed at 60% amplitude for 4 hrs. The WS_2/CHP stock was prepared at 18 mg/ml in 30 ml of CHP using an amplitude of 50% for 2.5 hrs. All stock dispersions were left to stand overnight to allow large unstable aggregates to settle out before further processing.

The stock dispersions were centrifuged using a Hettich Mikro 220R both to remove any unexfoliated layered material and to fractionate the nanosheets by size. They were first centrifuged at a relatively high rate, ω = 14000 rpm, for 100 mins, giving dispersions containing only the smallest nanosheets present in each of the stocks. The supernatant was retained for analysis leaving a highly-concentrated wet sediment of larger nanosheets and unexfoliated crystallites. This sediment was extracted and re-dispersed in fresh solvent (or aqueous SC solution) by mild bath sonication (approx 30 mins, Branson 1510E-MT). The re-dispersed material was then centrifuged at ω = 9000 rpm for 100 mins, the supernatant extracted and the wet sediment re-dispersed as before. This supernatant was expected to contain nanosheets which are small but not as small as the 14000 rpm process described above. In addition, as before, the sediment would contain larger nanosheets and unexfoliated crystallites. This process was repeated successively for rotation rates of 5500 rpm, 4000 rpm, 3000 rpm, 2000 rpm, 1000 rpm, 750 rpm and 500 rpm. We expect this to yield a set of dispersions with successively larger nanosheets. Different rotors were used depending on the rotation speed: a 24-way rotor (87 mm radius) holding 1.5 ml polypropylene microcentrifuge tubes was used for rotation rates (ω) above 6000 rpm (cooling at 10 °C to prevent

degradation of the tubes). For 500 rpm – 6000 rpm a 6-way rotor was used with samples placed inside 14 ml glass vials.

For all dispersions, samples for TEM were deposited on holey carbon grids by drop casting. TEM analysis was carried out with a Jeol 2100 operated at 200 kV. From initial TEM analysis it was observed that the graphene/NMP and MoS_2/NMP samples prepared at 14000 rpm had a small population of large nanosheets (excess 1 μm in lateral size). This was attributed to poor separation of supernatant and sediment in the microcentrifuge tubes used. To obtain a better separation, the supernatants prepared at ω = 14000 rpm and 9000 rpm for all four sample sets were re-centrifuged at the same rotation rate for a further 100 mins to remove any large nanosheets. UV-vis absorption spectra were recorded using a Varian Cary 6000i, with previously measured extinction coefficient values used to determine sample concentrations.[7, 9, 27]

DLS measurements were made with a Malvern Zetasizer Nano ZS, using a 633 nm HeNe laser. Samples were tested in stoppered glass or quartz cuvettes having 10 mm path length. The machine was operated in backscatter mode at an angle of 173°. Samples were equilibrated to 25 °C for 120 s prior to measurement. Values for solvent viscosity at 25 °C, as provided by the solvent suppliers, were entered into the software. An automatic measurement duration setting was used, with automatic measurement positioning and automatic attenuation. The samples were analysed as prepared without further dilution.

3. Results and Discussion

The first stage of this work was to prepare nanosheet dispersions for testing. This was achieved using recently developed methods for the liquid exfoliation of layered crystals.[7, 21, 23, 28, 47] Such methods involve the sonication of layered material in a suitable liquid and generally yield large quantities of relatively defect free nanosheets. As we aim to develop a general method for lateral size measurement, we have exfoliated three different layered materials, graphite (to give graphene), MoS_2 and WS_2. The graphite was exfoliated in both a solvent (NMP) and an aqueous surfactant solution while the MoS_2 and WS_2 were exfoliated in solvents (NMP and CHP respectively). These dispersions were then size-separated using controlled centrifugation[15, 47] at 9 different rotation rates, giving a total of 36 samples. These samples were then analysed using TEM and DLS.

Figure 1 shows a selection of bright field TEM images of the nanosheets studied in this work. Figure 1A shows a typical graphene nanosheet prepared in NMP. To determine nanosheet lateral dimensions, the shape of the nanosheet was approximated as rectangular, length measurements were taken along the major axis as illustrated by the dashed line in Figure 1A. In some cases clear folding of nanosheets was visible as shown by the graphene/SC nanosheet in Figure 1B. In these cases the total unfolded lengths of the nanosheets were estimated as shown by the dashed line. For some samples high areal coverage of the TEM grids was observed, this is shown in Figure 1C for a MoS_2 sample prepared at 14000 rpm in NMP. Some aggregation due to the drop-casting was observed, this is illustrated by the cluster of randomly aggregated WS_2 nanosheets in Figure 1D. By careful examination of the contrast between overlapping nanosheets the lengths can be measured.

For almost all samples the lengths of a minimum of 200 nanosheets were measured from TEM images. However, for some of the highest rotation rate samples the areal coverage of the TEM grids was too low and reliable statistics could not be derived; these samples were graphene/SC 14000 rpm, MoS_2/NMP 9000 rpm, WS_2/CHP 9000 rpm and WS_2/CHP 14000 rpm. However, this still resulted in at least 7 length measurements for each nanosheet type.

Figure 2 plots the distribution of measured nanosheet sizes, for dispersions prepared at ω = 750 rpm and ω = 5500 rpm, for each of the four systems analysed. It is immediately obvious that dispersions prepared at high rotation rate contain flakes which are much smaller than those in the lower rotation rate samples, in line with previous work.[15, 27, 47]. Figures 2A and 2B show broadly similar size distributions for exfoliated graphene dispersed in NMP and SC, respectively. Data for the inorganic layered materials, MoS_2 and WS_2, are shown in Figures 2C and 2D. The overall length distribution at both high and low rpm is shifted to smaller values compared to graphene. There are two reasons for this. First, exfoliated nanosheets of MoS_2 and WS_2 tend to be small compared to graphene nanosheets partly due to their lower strength.[7, 47] Secondly, the higher density of the inorganic nanosheets results in a larger centrifugal force being applied during the centrifugation process.[49] This may result in smaller nanosheets being retained at a given rotation rate compared to graphene.

To examine the overall change of nanosheet size with centrifugation rate, the mean nanosheet size, $\langle L \rangle$, can be plotted as a function of ω for all samples, as shown in Figure 3. In all cases the mean nanosheet length falls off with increasing centrifuge speed, showing that

controlled centrifugation can be used to tune nanosheet sizes. An empirical trend of $\langle L \rangle \sim \omega^{-0.6}$ is observed across the whole data range which agrees well with previous work.[15]

Having determined nanosheet sizes from TEM analysis we proceeded to analyse the samples with DLS. Dynamic light scattering probes the Brownian motion of the particles in a liquid suspension under conditions of constant temperature. The DLS instrument monitors the spatial intensity distribution of light scattered by a given sample as a function of time. This distribution constantly fluctuates as particles diffuse through the liquid. By measuring the auto-correlation of the intensity distribution as a function of time, information can be obtained about the motion of the particles. From this, the translational diffusion coefficient, *D*, of the particles can be calculated.[46] In general a particle moves through the liquid medium surrounded by a static fluid layer that is at rest with respect to the particle.[50, 51] The size of particle and fluid layer controls the hydrodynamic radius of the particle, *a*.[50] For a spherical particle, the hydrodynamic diameter and translational diffusion coefficient are related by the Stokes-Einstein equation:

$$D = \frac{kT}{6\pi\eta a} \qquad (1)$$

where η is the liquid viscosity.

In this study a commercially available Malvern Zetasizer Nano ZS was used. By operating in backscatter mode (173° scattering angle) it was possible to use the machine's automatic beam positioning system. This system optimises the focal position and attenuation of the incident beam prior to data acquisition.[52] Using these settings meant that the sample could be probed close to the cuvette wall, thus minimising multiple scattering of the light by highly concentrated samples. Hence, for this study, the samples did not need to be diluted in order to record size data. The DLS software uses a set of algorithms to analyse the correlation of scattering events and outputs the relative intensity of light scattered by particles of a given *a* value. This distribution of particle sizes is referred to as an intensity particle size distribution (PSD). Examples of typical intensity PSDs produced for graphene dispersions are given in Figure 4. For most samples a distribution similar to Figure 4A (graphene/NMP at ω = 1000 rpm) was observed. This distribution is characterised by a bell-shaped curve centred on a single peak value. Figure 4B shows the intensity PSD for a graphene/SC sample at ω = 5500 rpm, displaying a multi-peak distribution typical of a few of the samples. In this

case, a small peak around 28 nm is observed; this could be attributed to the presence of very small graphene nanosheets or a small population of amorphous carbon contaminants in the sample. However, the primary peak of the distribution is centred at 152 nm which agrees well with the length distribution from TEM analysis shown in Figure 2B. A third very small peak is observed at around 5 μm, this feature appeared in some samples. The origin of this peak is unclear as no large objects around 5 μm in size were observed during TEM analysis. However, this feature may be due to small dust particles or air bubbles in the dispersion.

In order to measure nanosheet size using DLS, an output from the instrument must be selected for comparison with the lateral size data measured with TEM. The main data output from the DLS instrument is the intensity PSD, requiring only knowledge of the solvent viscosity η as per equation 2, to derive size information. It is worth noting that the DLS software can use Mie theory to convert the intensity PSD to a volume PSD or number PSD. The conversion uses a user-programmed refractive index value for the particles to create distributions based on the physical volume or number of scattering particles; note that for volume PSD calculations the particles are assumed to be spherical. This method can be useful for systems of spherical particles where multiple intensity PSD peaks are observed. However, exfoliated layered compounds are clearly not spherical and the refractive index may not be precisely known. In addition, the spurious peaks of the type seen in Figure 4B were found to strongly distort the conversion for our systems. The DLS software also computes an averaged particle size value known as the "z-average diameter". This value is derived from the entire intensity PSD and so is also strongly influenced by the presence of any spurious peaks of the type shown in Figure 4B. In order to reduce these types of errors and inconsistencies, size information was derived from the intensity PSD.

For this study the primary peak position from the intensity PSD was used, this value will be referred to as a_{DLS}. Figure 5 plots a_{DLS} versus $\langle L \rangle$ for all four nanosheet systems tested. The a_{DLS} values across the four sample nanosheet systems sit on top of each other and scale linearly with $\langle L \rangle$ on this log-log graph. This implies that a_{DLS} is related to $\langle L \rangle$ by a power law. Fitting the data to $a_{DLS} = \alpha \langle L \rangle^{\delta}$, gave the exponent as $\delta = 0.66 \pm 0.06$ and $\alpha = 5.9 \pm 2.2$.

To understand the observed trend we note that for non-spherical particles, the hydrodynamic radius, a, is often approximated (this approximation effectively means neglecting the geometric frictional coefficent) as the radius of a sphere of volume equal to the

volume of the particle.[50, 53] Then, approximating the nanosheets as discs with thickness *t* and length (diameter) *L* allows us to write

$$a = \left(\frac{3}{16}\right)^{1/3} t^{1/3} L^{2/3} \quad (2)$$

Assuming that $a_{DLS} \sim a$ and that the thickness of the graphene, MoS_2 and WS_2 nanosheets are similar implies that, in our case; $a_{DLS} \propto L^{2/3}$. This is almost exactly what is found empirically in Figure 5. The fact that the data for the different nanosheets types fall on the same line supports this analysis as it shows that only nanosheets lateral dimension and not material type affects the value of *a* outputted by the DLS instrument.

This means that lateral nanosheet size can be estimated by DLS via a simple manipulation of the measured peak intensity PSD. Using the fit data from Figure 5, we can write

$$\langle L \rangle = (0.07 \pm 0.03) a_{DLS}^{(1.5 \pm 0.15)} \quad (3)$$

This expression can be used to estimate the mean nanosheet length from DLS data. We believe this could be a useful technique for estimating mean size of dispersed nanosheets. The alternative method of direct imaging using TEM or AFM is extremely time and labour intensive. In contrast, DLS offers a facile and fast method to estimate mean nanosheet sizes in liquid-phase dispersions.

However, it is important to note the limitations of this method. Firstly, the constants in expression 3 have relatively large uncertainties. This means that unless this calibration is improved upon, this method is unsuited to projects where accurate size values are required. In addition, this method can only reliably estimate the mean size of the nanosheets but not the size distribution. The distribution of nanosheet sizes cannot be reliably assessed as the DLS instrument derives a non-linear intensity PSD, this is a limitation of the instrument (see x-axis of Figure 4 for data point increments). This type of data output also limits the sensitivity of the technique to small changes in mean nanosheet size, particularly where the mean nanosheet size exceeds 1 μm Above this value the data points in the intensity PSD become spaced over large increments of size. In addition, the Malvern Zetasizer Nano ZS used in this study can only measure sizes over a limited range – from a few nm to ~10 μm. However, it is worth noting that most exfoliated nanosheets exist in this range. Finally, it was found that the

size data from very low concentration dispersions (absorbance per unit path length < 0.001 m^{-1}) was unreliable. This was due to the low number of scattering events and was flagged by the software under its built-in measurement quality reporting.

4. Conclusions

We have developed a simple method to estimate the lateral dimensions of nanosheets dispersed in a liquid. To do this we used centrifugation-based size selection methods to prepare dispersions of graphene, MoS_2 and WS_2 in different liquids with a range of different nanosheet sizes. In all cases the lateral nanosheet sizes were measured using TEM. The same set of dispersions were characterised by dynamic light scattering using a common commercial instrument. We found the size value outputted by the light scattering instrument scaled very well with the measured nanosheet length. This allows us to generate a semi-empirical expression relating the nanosheet length to the DLS output.

This method can be used to get a reasonable estimate (relative error 40%) of the lateral size of any 2-dimensional nanosheets dispersed in a liquid. It is fast, simple and used equipment available in most analytical labs. While it is not highly accurate it is perfectly suited to preliminary measurements or comparison of samples where a large size differential is expected.

Acknowledgements

The authors would like to acknowledge Science Foundation Ireland, (grant numbers 07/IN.7/I1772, 08/IN.1/I1862), and ERC grant SEMANTICS for financial support.

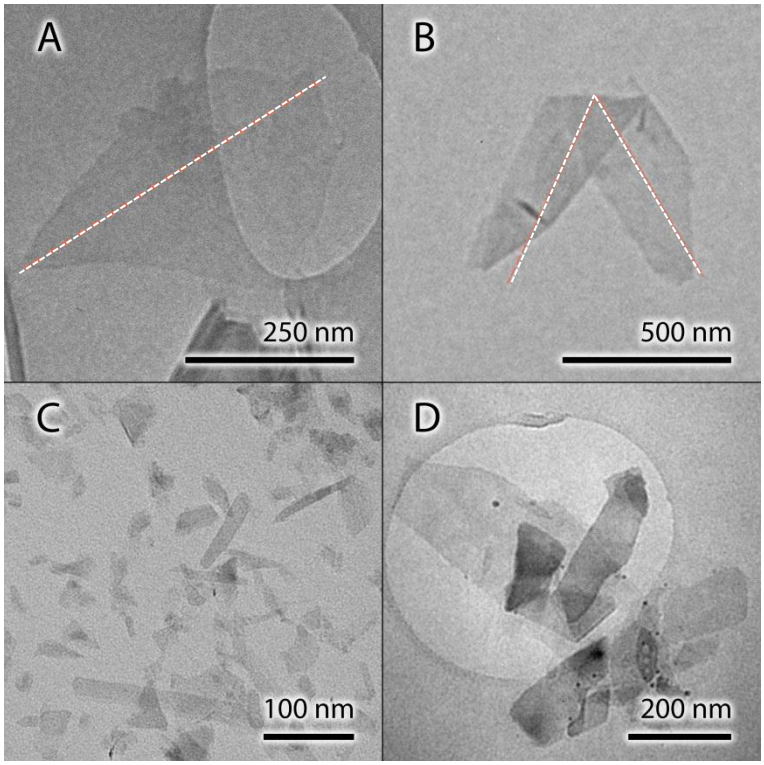

Figure 1: Bright field TEM images of nanosheets from size-selected dispersions. (A) Graphene/NMP at 3000 rpm. (B) Graphene/SC at 500 rpm. (C) MoS_2/NMP at 14000 rpm. (D) WS_2/CHP at 5500 rpm. Dashed lines in A and B illustrate the method used to determine nanosheet lateral sizes.

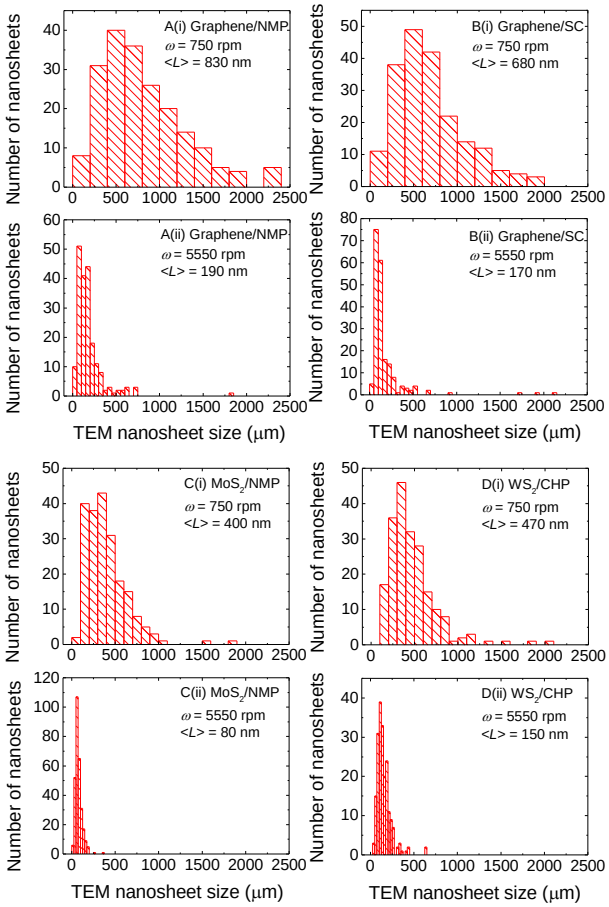

Figure 2: Histograms of measured nanosheet size at centrifuge rates, ω, of 750 rpm and 5500 rpm for (A) graphene/NMP, (B) graphene/SC, (C) MoS_2/NMP, (D) WS_2/CHP

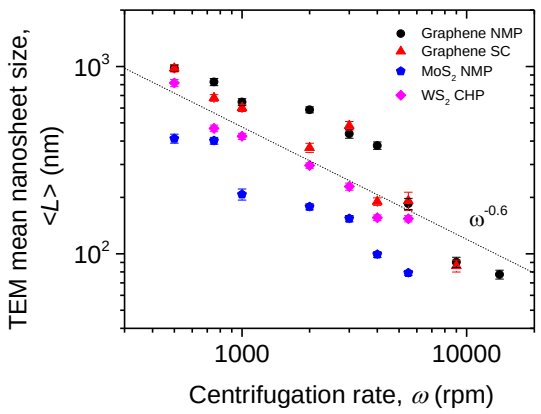

Figure 3: Mean nanosheet length, <*L*>, versus centrifugation rate, ω, for all samples studied. Error bars show standard error of <*L*>. The dashed line illustrates $\omega^{-0.6}$ behaviour.

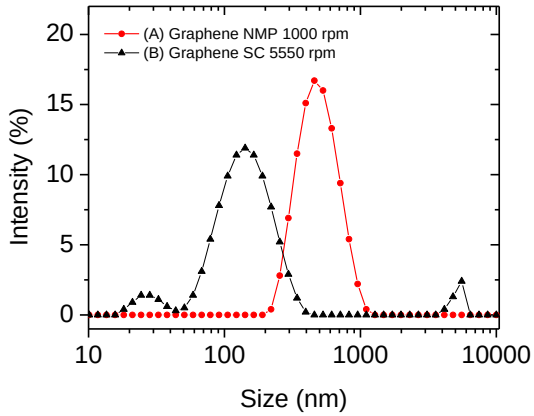

Figure 4: Intensity particle size distribution for graphene nanosheets in A) NMP at 1000 rpm and B) SC solution at 5500 rpm.

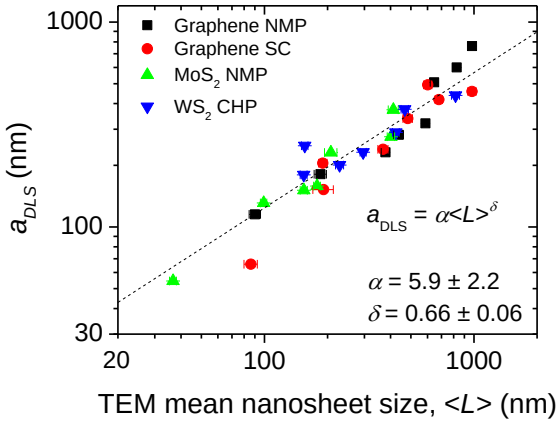

Figure 5: Primary intensity PSD peak position, a_{DLS}, versus mean nanosheet size, $\langle L \rangle$, measured from TEM image analysis. Dashed line: fitted power law dependence of a_{DLS} with $\langle L \rangle$

References

1. Novoselov KS, Fal'ko VI, Colombo L, Gellert PR, Schwab MG, Kim K 2012 *Nature* 490 192-200
2. Osada M, Sasaki T 2009 *Journal of Materials Chemistry* 19 2503-11
3. Wang QH, Kalantar-Zadeh K, Kis A, Coleman JN, Strano MS 2012 *Nature Nanotechnology* 7 699-712
4. Mak KF, He K, Lee C, Lee GH, Hone J, Heinz TF, et al. 2013 *Nat Mater* 12 207-11
5. Radisavljevic B, Radenovic A, Brivio J, Giacometti V, Kis A 2011 *Nature Nanotechnology* 6 147-50
6. Novoselov KS, Geim AK, Morozov SV, Jiang D, Zhang Y, Dubonos SV, et al. 2004 *Science* 306 666-9
7. Coleman JN, Lotya M, O'Neill A, Bergin SD, King PJ, Khan U, et al. 2011 *Science* 331 568-71
8. Khan U, May P, O'Neill A, Bell AP, Boussac E, Martin A, et al. 2013 *Nanoscale* 5 581-7
9. Hernandez Y, Nicolosi V, Lotya M, Blighe FM, Sun ZY, De S, et al. 2008 *Nature Nanotechnology* 3 563-8
10. Blake P, Brimicombe PD, Nair RR, Booth TJ, Jiang D, Schedin F, et al. 2008 *Nano Letters* 8 1704-8
11. Bourlinos AB, Georgakilas V, Zboril R, Steriotis TA, Stubos AK 2009 *Small* 5 1841-5
12. Hamilton CE, Lomeda JR, Sun ZZ, Tour JM, Barron AR 2009 *Nano Letters* 9 3460-2
13. Hasan T, Torrisi F, Sun Z, Popa D, Nicolosi V, Privitera G, et al. 2010 *Physica Status Solidi B-Basic Solid State Physics* 247 2953-7
14. Choi EY, Choi WS, Lee YB, Noh YY 2011 *Nanotechnology* 22
15. Khan U, O'Neill A, Porwal H, May P, Nawaz K, Coleman JN 2012 *Carbon* 50 470-5
16. Keeley GP, O'Neill A, McEvoy N, Peltekis N, Coleman JN, Duesberg GS 2010 *Journal of Materials Chemistry* 20 7864-9
17. Liang YT, Hersam MC 2010 *Journal of the American Chemical Society* 132 17661-3
18. Nuvoli D, Valentini L, Alzari V, Scognamillo S, Bon SB, Piccinini M, et al. 2011 *Journal of Materials Chemistry* 21 3428-31
19. Zhang XY, Coleman AC, Katsonis N, Browne WR, van Wees BJ, Feringa BL 2010 *Chemical Communications* 46 7539-41
20. Alzari V, Nuvoli D, Scognamillo S, Piccinini M, Gioffredi E, Malucelli G, et al. 2011 *Journal of Materials Chemistry* 21 8727-33
21. Cunningham G, Lotya M, Cucinotta CS, Sanvito S, Bergin SD, Menzel R, et al. 2012 *Acs Nano* 6 3468–80
22. Hernandez Y, Lotya M, Rickard D, Bergin SD, Coleman JN 2010 *Langmuir* 26 3208-13
23. Khan U, O'Neill A, Lotya M, De S, Coleman JN 2010 *Small* 6 864-71
24. Zhou K-G, Mao N-N, Wang H-X, Peng Y, Zhang H-L 2011 *Angewandte Chemie International Edition* 50 10839-42
25. Notley SM 2012 *Langmuir* 28 14110-3
26. Lotya M, Hernandez Y, King PJ, Smith RJ, Nicolosi V, Karlsson LS, et al. 2009 *Journal of the American Chemical Society* 131 3611-20
27. Lotya M, King PJ, Khan U, De S, Coleman JN 2010 *Acs Nano* 4 3155-62
28. Smith RJ, King PJ, Lotya M, Wirtz C, Khan U, De S, et al. 2011 *Advanced Materials* 23 3944-8
29. Green AA, Hersam MC 2009 *Nano Letters* 9 12
30. Hao R, Qian W, Zhang LH, Hou YL 2008 *Chemical Communications* 6576-8
31. Vadukumpully S, Paul J, Valiyaveettil S 2009 *Carbon* 47 3288-94

32. Bourlinos AB, Georgakilas V, Zboril R, Steriotis TA, Stubos AK, Trapalis C 2009 *Solid State Commun* 149 2172-6
33. May P, Khan U, Hughes JM, Coleman JN 2012 *Journal of Physical Chemistry C* 116 11393-400
34. Coleman JN 2013 *Accounts of Chemical Research* 46 14-22
35. Shih CJ, Vijayaraghavan A, Krishnan R, Sharma R, Han JH, Ham MH, et al. 2011 *Nature Nanotechnology* 6 439-45
36. Zeng ZY, Yin ZY, Huang X, Li H, He QY, Lu G, et al. 2011 *Angewandte Chemie-International Edition* 50 11093-7
37. Eda G, Yamaguchi H, Voiry D, Fujita T, Chen MW, Chhowalla M 2011 *Nano Letters* 11 5111-6
38. Dreyer DR, Ruoff RS, Bielawski CW 2010 *Angewandte Chemie-International Edition* 49 9336-44
39. Park S, Ruoff RS 2009 *Nature Nanotechnology* 4 217-24
40. May P, Khan U, O'Neill A, Coleman JN 2012 *Journal of Materials Chemistry* 22 1278-82
41. Stankovich S, Dikin DA, Dommett GHB, Kohlhaas KM, Zimney EJ, Stach EA, et al. 2006 *Nature* 442 282-6
42. Huang HD, Ren PG, Chen J, Zhang WQ, Ji X, Li ZM 2012 *Journal of Membrane Science* 409 156-63
43. Barth HG, Flippen RB 1995 *Analytical Chemistry* 67 257-72
44. Wyatt PJ 1998 *Journal of Colloid and Interface Science* 197 9-20
45. Giddings J, Yang F, Myers M 1976 *Science* 193 1244-5
46. Badaire S, Poulin P, Maugey M, Zakri C 2004 *Langmuir* 20 10367-70
47. O'Neill A, Khan U, Coleman JN 2012 *Chemistry of Materials* 24 2414-21
48. Zhi C, Bando Y, Tang C, Kuwahara H, Golberg D 2009 *Advanced Materials* 21 2889-93
49. Nicolosi V, Vrbanic D, Mrzel A, McCauley J, O'Flaherty S, McGuinness C, et al. 2005 *Journal of Physical Chemistry B* 109 7124-33
50. Atkins PW, Paula JD. Physical Chemistry. Oxford: W.H. Freeman; 2006.
51. Phillies GDJ 1981 *The Journal of Physical Chemistry* 85 2838-43
52. Frindt RF 1965 *Physical Review* 140 A536
53. van Holde KE. Physical biochemistry. Englewood Cliffs: Prentice-Hall; 1971.